Proceedings of the ASME 2010 3rd Joint US-European Fluids Engineering Summer Meeting and 8th International Conference on Nanochannels, Microchannels, and Minichannels
FEDSM-ICNMM2010
August 1-5, 2010, Montreal, Canada

FEDSM-ICNMM2010-30322

ACTIVE CONTROL OF AIR FLOW IN VEHICLE UNDERHOOD COMPARTMENT-TEMPERATURE AND HEAT FLUX ANALYSIS

Mahmoud Khaled
Thermofluids, Complex Flows and Energy Research Group – Laboratoire de Thermocinétique, CNRS-UMR 6607, Ecole Polytechnique
University of Nantes
Nantes, France

Fabien Harambat
Aerodynamic and Aeroacoustic Research and Development Department – PSA Peugeot Citroen
Vélizy, France

Anthony Yammine
Testing System and Turbocharging Department – Kratzer Automation
Jouy en Josas, France

Hassan Peerhossaini
Thermofluids, Complex Flows and Energy Research Group – Laboratoire de Thermocinétique, CNRS-UMR 6607, Ecole Polytechnique
University of Nantes
Nantes, France

ABSTRACT
An experimental analysis of the aerothermal phenomena in the vehicle underhood is given using temperature measurements and separate measurements of convective and radiative heat fluxes. The vehicle underhood used for these measurements is instrumented by 120 surface and air thermocouples and 20 fluxmeters. Measurements are carried out on a passenger vehicle in wind tunnel S4 of Saint-Cyr-France for three thermal functioning conditions. In particular, it is shown for some components that outside air entering the engine compartment (for cooling the different components by convection) can in fact heat other components. This problem results from the underhood architecture, specifically the positioning of some components downstream of warmer components in the same airflow. To avoid this undesired situation, an optimized thermal management procedure is proposed that uses static and dynamic air deflectors during the constant-speed driving (rooting) phase of a vehicle. Much of the present paper is devoted to fluxmetric analysis of underhood thermal behavior (especially the absorption of convective heat flux); we also describe a new control procedure for implementing air deflectors in the actual car underhood.

Keywords: Temperature and heat flux measurements, Convective heat flux, Radiative heat flux, Underhood aerothermal management, Static and dynamic air deflectors, Physical analysis, Active control.

INTRODUCTION
Increasing crowding in the vehicle underhood compartment has made it the seat of complex aerothermal phenomena, especially convection and radiation, with complicated airflows and difficult air paths. Experimental analyses of these phenomena [1-4] are rare and studies focus mainly on numerical simulations [5-10], which themselves concentrate primarily on temperature analysis. It should also be noticed that existing experimental work on underhood studies give very little physical analysis of heat transfer, and mainly comment on the comparisons between

computations and experiments [11-15]. On the other hand, the underhood geometry is already so confined and complex that it is difficult to redesign; the remaining approach is to seek to optimize the aerothermal properties by acting on its operation mode rather than its architecture.

The present paper gives a physical analysis of particular underhood aerothermal behaviors on which to base a new optimization approach [16] that redistributes cooling airflow in the vehicle underhood compartment. First an experimental study of the aerothermal phenomena encountered in the vehicle underhood is presented as assessed by temperature measurement and separate measurements of convective and radiative heat fluxes. Measurements are carried out on a passenger vehicle in wind tunnel S4 of Saint-Cyr-France. The underhood is instrumented by 120 surface and air thermocouples and 20 fluxmeters. Measurements are performed for three thermal functioning conditions, the engine in operation and the front wheels positioned on the test facility with power-absorption rollers. Then the optimization approach, which is based on the physical analysis and involves using static and dynamic deflectors to direct different air flow paths in the underhood,, is presented.

The rest of this article is organized as follows. The next section, describes the experimental setup. In the following section the temperature and heat flux measurements are analyzed, and the final section is devoted to new control procedures for optimization of the underhood aerothermal management.

EXPERIMENTAL SETUP

In this section, the instrumentation of the underhood and the test configurations are described [17-20].

Underhood instrumentation

The underhood of the vehicle used in the experiments is instrumented by type T and K surface and air thermocouples and fluxmeters of normal gradients. Thermocouples permit temperature measurements at almost 120 positions corresponding to different components, air zones and engine parameters (engine fluid characteristic temperatures). Fluxmeters are attached to the surfaces in pairs (20 fluxmeters in 10 positions) so as to make separate measurement of the convective and radiative heat fluxes. This technique, described in [21-23], entails attaching to a surface of given emissivity two fluxmeters of different emissivities (a way to do this in practice is to paint one fluxmeter with black paint and the other with aluminum paint). In this case, the overall heat fluxes measured by the two fluxmeters are not the same. By considering the surface temperatures and the convective heat transfer coefficient measured by the two fluxmeters to be approximately the same, one can deduce from the overall heat fluxes measured by the two fluxmeters the convective and radiative heat flux exchanged at the surface.

Among the components tested, the most important are the exhaust manifold, the cold box (the box protecting the vehicle calculator and battery), the alternator, the admission distributor, the air filter, the water outlet plenum, the apron, the charge air cooler (CAC) inlet and outlet ducts, the cylinder head cover and the right side of the engine. Among the air zones, the most important are those close to the cowl, the apron, the cold box, the cylinder head cover, the air filter, the CAC inlet and outlet ducts and that downstream of the engine and the charge air cooler. Engine parameters are temperatures: of water at the radiator inlet and outlet, of air at the charge air cooler and compressor inlet and outlet, of gas at the turbine and catalyzer inlet and outlet and of air at the engine (cylinders) inlet. Figure 1 shows a schematic of the instrumentation locations in the underhood (top and side views) and an example of instrumentations at the cold box.

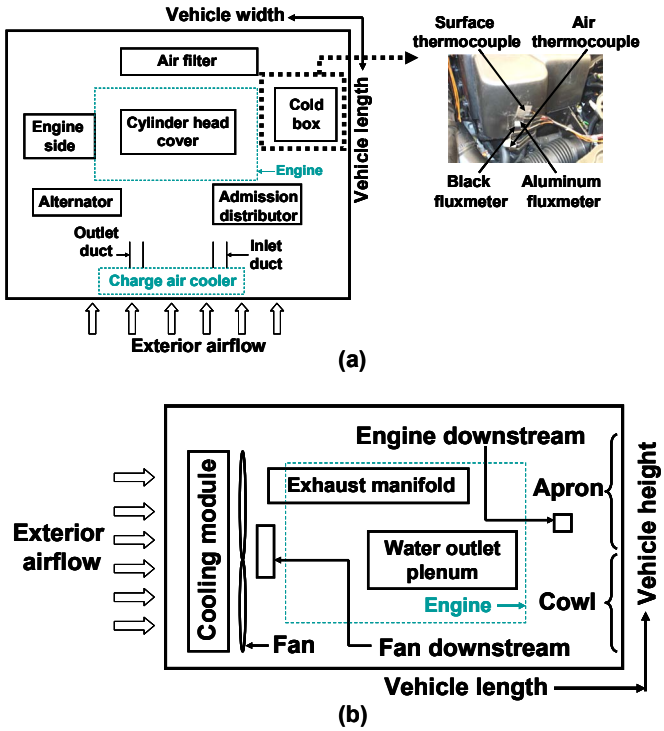

Figure 1: Schematic of (a) top and (b) side views of some instrumented underhood locations.

Test configurations

Aerothermal tests were performed in the wind tunnel S4 of Saint-Cyr l'Ecole France. There is a 1:1 wind tunnel with a 5 m wide and 3 m high section. Walls filled with a vein of this size cause changes in the flow around a vehicle at scale 1. To mitigate these effects, blower S4 has a ventilated vein-type with

longitudinal cracks that make the flow very close to the real flow around the vehicle. In addition, the wind tunnel has a rollers chassis that can put rolling resistance on the vehicle. Thus, it is possible to conduct tests with the wheels rotating and driven by the engine speed and linked to the roller. The front wheels are placed on the chassis roller. The car engine is running during the tests, and the vehicle driver accelerates and the front wheels then entrain the rolls. The roller test facility is equipped with a brake system to adjust and control the power to the wheels and their rotational speed (Figure 2).

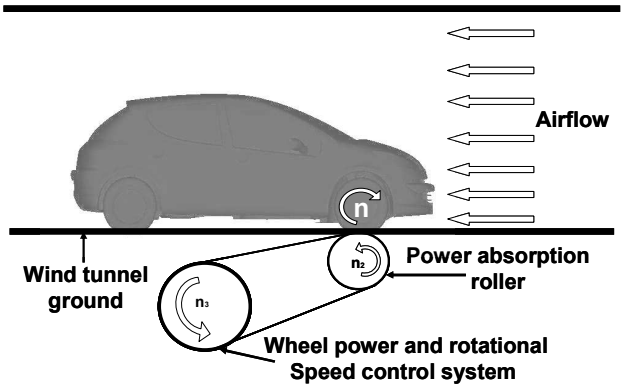

Figure2: Roller test facility equipments

Tests were carried out for three different thermal functioning points that simulated more or less severe rolling situations from the thermal point of view (Table 1).

	V_{wheel} Km.h^{-1}	V_{wind} Km.h^{-1}	P kW	R -	n rpm
PT-FCT-1	90	90	69	5	2600
PT-FCT-2	110	55	89	4	3800
PT-FCT-3	130	130	98	5	3780

Table 1: Parameters defining the three thermal functioning points: wheel and wind speeds, engine power, gearbox ratio and engine regime.

For each test, data records cover three successive phases, each simulating real situations with which a vehicle can be confronted: constant-speed driving (at a thermal functioning point defined by one of the three points in table 1), slowdown and thermal soak (thermal soak follows slowdown and simulates stopping the vehicle after a significant heat load).

RESULTS AND ANALYSIS

Analyses of temperature and heat flux measurements are given below in two parts: underhood thermal behavior description and heat flux analysis by separate convective and radiative flux measurements.

Underhood thermal behaviors

During the constant-speed driving phase and for the different thermal functioning points, typical exponential trends are observed in all component temperature variations, air zones and engine parameters. Exponential trends are also obtained for the temporal variation of overall, convective and radiative heat fluxes for all components tested. Examples of exponential tendencies are shown in Figure 3 and Figure 4, for thermal point TFP-1: for the temperature and overall heat flux in Figure 3 and for convective and radiative heat fluxes in Figure 4. In Figures 3 and 4, the different heat flux curves are made dimensionless, by the initial flux for decreasing flux and by the final (infinite) flux for increasing flux.

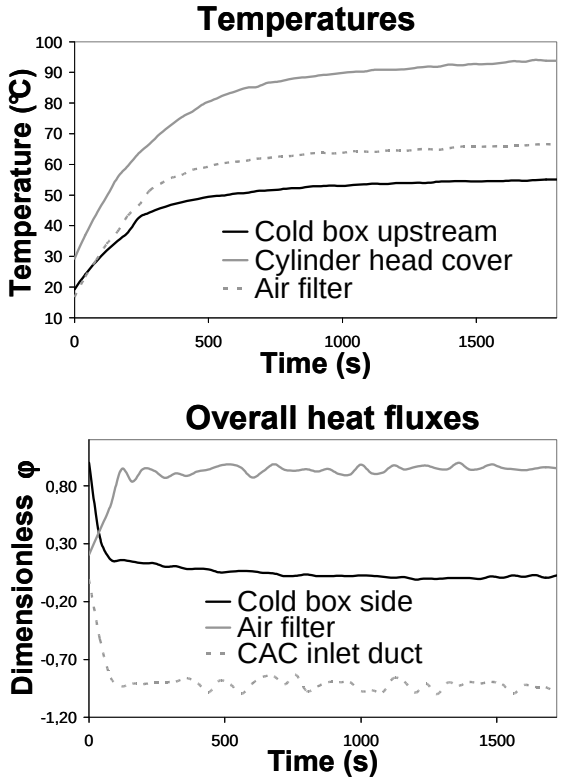

Figure 3: Examples of temperature and overall heat flux variation for some components in TFP-1.

Temperature-time variations in the constant-speed driving phase systematically follow the general form:

$$T(t) = T_0 + (T_{\max} - T_0).\left[1 - \exp\left(-\frac{t}{\tau}\right)\right] \qquad (1)$$

Here $T_{\max}$ is the maximum temperature of quasi-stabilization at the end of the constant-speed phase and τ is the time constant, i.e. the typical time to attain the stabilization regime.

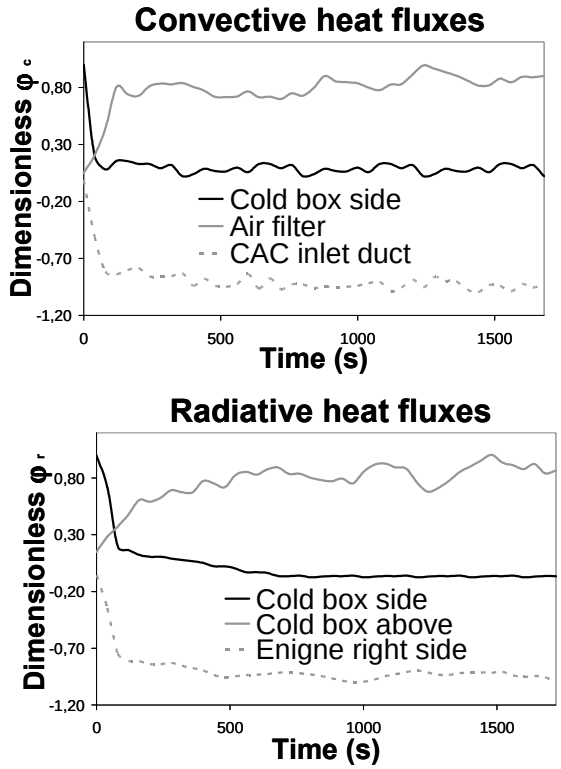

Figure 4: Examples of convective and radiative heat flux variation for some components in TFP-1.

The typical exponential expressions describing the overall, convective and radiative heat fluxes in the constant-speed driving phase are:

$$\varphi = \varphi_0 + (\varphi_{\max} - \varphi_0).\left[1 - \exp\left(-\frac{t}{\tau}\right)\right] \quad (2)$$

$$\varphi = \varphi_\infty + (\varphi_0 - \varphi_\infty).\exp\left(-\frac{t}{\tau}\right) \quad (3)$$

$$\varphi_c = \varphi_{c,0} + (\varphi_{c,\max} - \varphi_{c,0}).\left[1 - \exp\left(-\frac{t}{\tau}\right)\right] \quad (4)$$

$$\varphi_c = \varphi_{c,\infty} + (\varphi_{c,0} - \varphi_{c,\infty}).\exp\left(-\frac{t}{\tau}\right) \quad (5)$$

$$\varphi_r = \varphi_{r,0} + (\varphi_{r,\max} - \varphi_{r,0}).\left[1 - \exp\left(-\frac{t}{\tau}\right)\right] \quad (6)$$

$$\varphi_r = \varphi_{r,\infty} + (\varphi_{r,0} - \varphi_{r,\infty}).\exp\left(-\frac{t}{\tau}\right) \quad (7)$$

Here φ_0, $\varphi_{c,0}$ and $\varphi_{r,0}$ are respectively the overall, convective and radiative heat fluxes measured for each position at the beginning of the constant-speed driving phase. $\varphi_{\max}$, $\varphi_{c,\max}$ and $\varphi_{r,\max}$ are the maximum values during the phase and φ_∞, $\varphi_{c,\infty}$ and $\varphi_{r,\infty}$ are the asymptotic values at which the quasi-stabilization regime is reached. All these heat fluxes can be either positive or negative depending on whether the components receives or gives up heat to its environment, and they are essentially functions of the component location and the thermal functioning point.

Figure 5 compares curves obtained from experimental data and the theoretical exponential curves. These comparisons concern the temperature variation at the cold box side, the overall heat flux variation at the CAC outlet duct, the convective heat flux variation at the CAC inlet duct and the radiative heat flux variation at the engine right side in TFP-1.

Figure 5 shows that the experimental variations in temperatures and heat fluxes fit well with the theoretical exponential tendencies. For example, at the cold box side, the mean difference between experimental and theoretical curves is 0.2°C (0.4%). At the CAC inlet duct, this difference in the convective heat flux is 0.4%, and it is 1% for the overall heat flux at the CAC outlet duct and 2% for the radiative flux at the engine right side. These relative differences in experimental and theoretical trends were observed for all positions tested and for the different thermal functioning points, confirming the typical exponential tendencies of temperature and heat flux (overall, convective and radiative) in constant-speed driving phase.

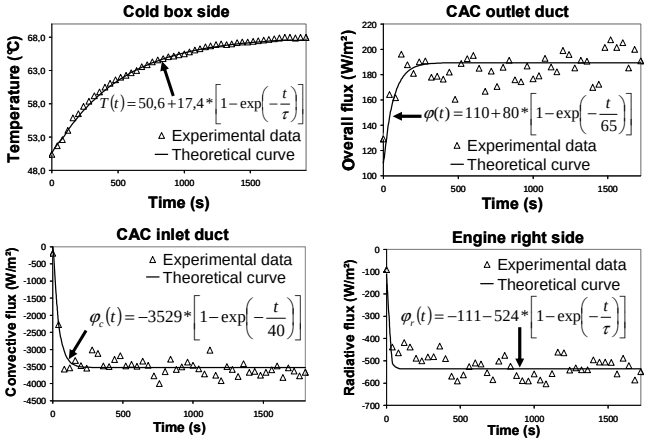

Figure 5: Comparisons between experimental data and theoretical curves for the temperature, overall flux, convective and radiative heat fluxes for some components.

For the overall heat flux variations, two categories can be distinguished:

- Category 1: components for which the overall heat flux follows the general form of equation (5). These are components that absorb or lose overall heat fluxes

increasing in absolute value with time. In other words, these components heat more slowly than their local thermal environment when they absorb heat or more quickly when they lose heat;

- Category 2: components for which the overall heat flux follows the general form of equation (6). These are components that absorb or lose overall heat fluxes decreasing in absolute value with the time. In other words, these components heat more quickly than their near thermal environment when they absorb heat or more slowly when they lose heat.

The same distinction in the variation of convective heat flux (equations (7), (8)) and radiative heat flux (equations (9), (10)) can be noticed. However, an overall heat flux variation of the first type does not necessarily arise from variations in the convective and radiative heat fluxes of the same category. For example, as seen in Figure 5 for the cold box component, the radiative heat flux increases in absolute value (category 1), unlike the overall and convective heat fluxes (category 2).

Fluxmetric analysis – components heated by convection

All components in the constant-speed driving phase absorb heat. But the surfaces of all components have at least one portion that receives heat and at least one that emits heat. Consider the first case, i.e. surfaces where the overall heat flux is absorbed (thus positive). Measurements show that there are particular cases where the convective heat flux is also positive. In other words, air that cools the different underhood components induces in some areas the opposite effect and tends to heat them. This is observed, for example, for the air filter or cold box (battery + calculator). Here the focus is on cases in which the components are heated by convection.

On the other hand, measurements show that for almost all components, the overall heat flux is driven by the convective heat flux, i.e. the time variation of the overall heat flux follows that of the convective heat flux, whatever the sign and intensity of the radiative flux. Then, two types of variations can be distinguished: increasing convective flux that imposes increased overall heat flux, and decreasing convective flux that induces decreased overall heat flux.

A typical example of the first type is the air filter. Figure 6 shows variations in the overall heat flux and temperatures on its surface and the surrounding air.

It can be clearly seen that the overall heat flux exchanged at the air filter surface is absorbed flux (+1350 W/m²). Indeed, at first the air zone near the air filter is hotter than its surface (Figure 5b): the passage of hot air that has extracted heat from components at high temperatures upstream of the air filter, especially the engine, provides then a positive (absorbed) convective flux (+500 W/m²). On the other hand, the radiative heat flux (+850 W/m²) is absorbed heat flux since the equivalent thermal environment of the air filter is hotter than its surface.

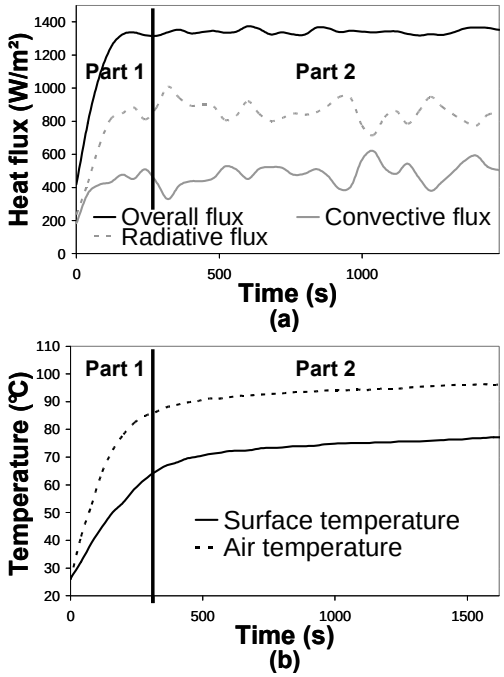

Figure 6: Temporal variations of (a) heat flux and (b) temperature at the air filter and surrounding air zone in TFP-3.

Moreover, it can be noticed that in the first part of the constant-speed driving phase, the temperature of the air zone surrounding the air filter increases faster than that of its surface (Figure 5b). This explains the increased absorbed convective heat flux (Figure 5a), the convective coefficient h_c remaining nearly constant since it is in a forced convection regime. In the second part of the constant-speed phase, the convective heat flux is stabilized because the difference between surface and air temperatures no longer varies.

Conversely, the radiative heat flux variation (Figure 5a) gives us information about the equivalent radiative temperature of the air filter thermal surrounding, T_r. This temperature increases faster than the surface temperature before becoming almost constant in the second part of the constant-speed phase, where T_S stabilizes ($T_r = \sqrt[4]{T_S^4 + (\varphi_r / \varepsilon.\sigma)}$).

A second typical example is the decreasing convective heat flux. Figure 7 shows data for the cold box.

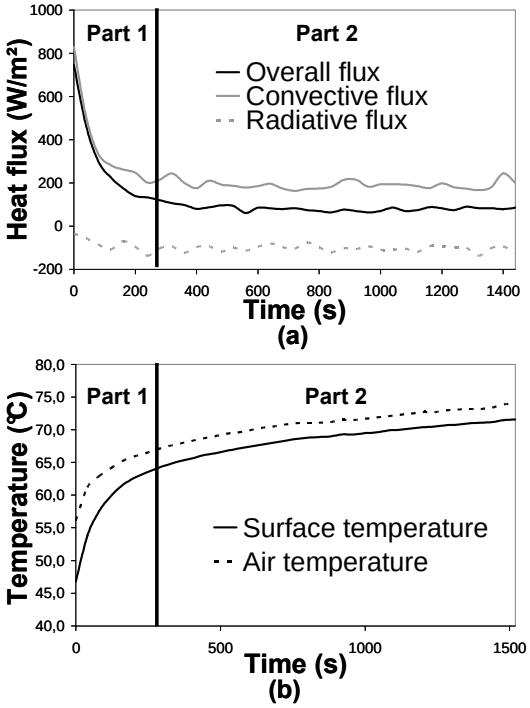

Figure 7: Temporal variations of (a) heat flux and (b) temperature at the cold box and surrounding air zone in TFP-3.

Again, the convective heat flux is positive because the surrounding air is heated near the components upstream of the cold box and its temperature becomes higher than that of the cold box. On the other side, convective heat flux decreases because this time the surface temperature increases more rapidly than that of the surrounding air zone (but remains below it), this decrease now being found in the overall heat flux with a shift due to the negative (emitted) radiative heat flux.

Finally, the examples above show that the exterior air that enters the underhood compartment to cool it by convection can induce the warming of some components, as shown by the cold box, which is a "critical" component from a thermal point of view since it contains computers. This problem is a result of the underhood actual architecture, specifically the positioning of these components in the same air flow as and downstream of warmer components. An optimized thermal design may be to place these components in areas further upstream or to isolate them form hot air flow using deflectors.

Note that in the case of decreasing convective heat flux, it is essentially the early part of the transitional curve that is problematic, since the convective heat flux can reach up to five times its asymptotic value. One can therefore imagine a mobile deflector that cuts off the air flux towards the component in the interim period only, letting pass the stabilized heat flux that might be useful for other components nearby or downstream. The deflector might even be bonded to a convective flux sensor.

The next section gives more details on deflectors based on the fluxmetric analysis discussed above.

UNDERHOOD AIR FLOW CONTROL BY DEFLECTORS

The present section describes a new underhood control approach in which static and mobile deflectors are placed in the underhood in order to protect certain components from hot air circulation. These deflectors can also direct warm air passing by low-temperature components to higher-temperature components for cooling. The procedures proposed here, which are simple and easily implemented in the car, are based on the physical analysis of the aerothermal phenomena obtained from our temperature and separate convective and radiative heat fluxes measurements. The deflectors proposed here may be connected to convective heat flux sensors [21-23].

Passive control by static deflectors

The passive version of the control uses deflectors positioned upstream of the components heated by convection. This procedure is in fact the optimization of the thermal management of components in one of the two typical cases of absorbed convective heat described in section 4.2, provided that the latter are in the rear part of the vehicle underhood. The control principle in this version is illustrated in Figure 8.

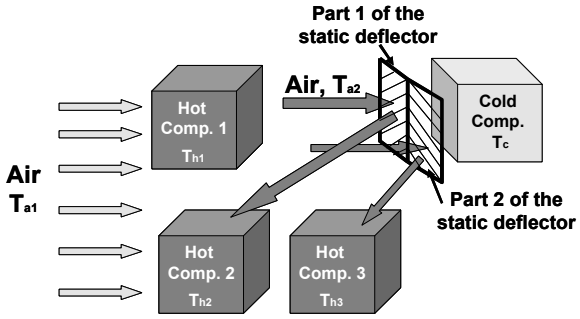

Figure7: Schematic of the static deflector principle.

In Figure 8, the temperature T_{a1} of air passing over the hot component 1 of temperature T_{h1} greater than the temperature T_c of the cold component rises to a temperature T_{a2} above temperature T_c. Without deflectors, the hot air induces a positive convective heat flux that increases the cold component's temperature. The first part of the static deflector guides a portion of the hot air flow of temperature T_{a2} (greater than T_c) towards the hot component 2 of temperature T_{h2} higher than T_{a2} and T_c. The second part of the deflector, on the other hand, directs a second portion of the hot air stream to the hot component 3 of temperature T_{h3}, also greater than T_{a2}

and T_c. Therefore, with the static deflector, one can transform a convective heat flux absorbed by a cold component on excesses of convective heat flux extracted by other components at higher temperatures. It should be noted that the static deflector can be in one part (or at one inclination) for a single hot component in its environment, or in more than one part (> 2) for many warm components in the environment.

Active control by dynamic deflectors

The active version of the control involves placing mobile (dynamic) deflectors upstream of components heated by convection. Repeating the two typical cases of convective heat absorption from the previous section, the active control can be used in two different applications: the first in which the deflector is closed during the transient part of the constant-speed driving phase and open during the stabilized part, and the second in which deflectors are open during the transient part and closed during the stabilized phase. The principle of the first application, "closed–open," is shown in Figure 9, where, 1 and 2 designate respectively the transitional and stabilized parts of the constant-speed driving phase. Monotony (increasing or decreasing heat flux) refers to the absolute values, not the algebraic values.

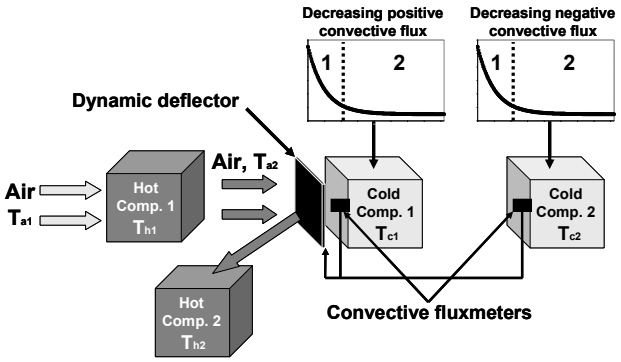

Figure 9: Schematic of the functioning principle of a closed-open dynamic deflector in the closed position in the transitory phase.

In the absence of deflectors, the first cold component absorbs convective heat flux more in the transitional than in the stabilized part, and the second cold component loses more convective heat in the stabilized than in the transitional part. To manage the thermal situation between the different components of Figure 10, the mobile deflector closes during the transitional stage and opens in the steady (stabilized) stage. In transition, it directs the hot air stream of temperature T_{a2} (which was heated by passing over the hot component 1 of temperature T_{h1} greater than T_{a1}) greater than T_{c1} and T_{c2} towards another hot component 2 of temperature T_{h2} still greater than T_{c1}, T_{c2} and T_{a2}. At the beginning of the stabilization, the deflector opens to let in the air needed for cooling cold component 2, which is not now critical for the cold component 1. Note that this application "closed–open" can be used only for a cold component that absorbs convective heat flux (positive) and is located upstream of other components that themselves evacuate convective heat flux (negative) increasing in absolute value with time. The mobile deflector is controlled by two heat flux sensors on the surfaces of both cold components in front of the air stream.

The principle of the second application, "open–closed," is shown in Figure 10.

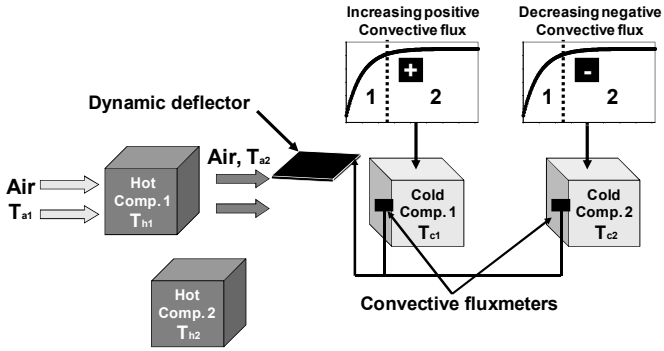

Figure 10: Schematic of the open–closed dynamic deflector principle in the open position and in the transitory phase.

In the absence of the deflector, the first cold component receives more convective heat flux in the stabilized phase than in the transitory regime, and the second cold component loses more convective heat in the transitory regime than in the stabilized regime. To manage the thermal situation of the different components of Figure 9, the mobile deflector opens during the transitory phase and closes during the stabilized phase. In the transitory part, the open deflector allows the passage of the air necessary to cool the cold component 2 even if the first cold component absorbs convective flux, provided that this latter is very small compared to what is evacuated by the second cold component.

At the transitory phase, the deflector closes in order to deviate the hot air, which heats the first cold component and is not very efficient in cooling the second cold component, towards the hot component 2 of temperature greater than those of the surrounding air and the two cold components. It should be noted that this "open–closed" application can be used only for a cold component that absorbs increased convective flux (positive) and is placed upstream of other components that themselves lose convective heat flux (negative) decreasing in absolute value with time.

In conclusion, one can optimize the underhood aerothermal management without changing the architecture or the positioning of components in the vehicle underhood. The technical interest of this control procedure resides in the fact

that it optimizes the cooling of underhood components that either either insufficiently cooled or are heated by convection due to the underhood architecture. On the other hand, the economic advantages of such optimized underhood aerothermal management (with or without active systems) are indirect:

- reduction of thermal crises, thus reducing warranty costs and expense related to possible emergency patches;
- better interaction with external aerodynamics: better management of the underhood air flow reduces the area of air inlet openings and thus aerodynamic drag (fuel consumption and carbon emission issues).

CONCLUSIONS

The present paper has given a physical analysis of particular underhood aerothermal behaviors, especially the convective heat flux absorption, and presents a new optimization procedure [16] based on this physical analysis and entailing the redistribution of cooling airflow in the vehicle underhood compartment.

During the constant-speed driving phase, for the different thermal functioning points investigated, typical exponential trends are observed in the temperature variations of all components, air zones and engine parameters. Exponential trends are also found for the temporal variation of overall, convective and radiative heat fluxes for all components investigated. For the overall heat flux variation (as well as for the convective and radiative parts), two component categories are distinguished: category 1, those components that absorb or lose overall heat fluxes increasing in absolute value with time, and category 2, those components that absorb or lose overall heat fluxes decreasing in absolute value with time.

On the other hand, it has been shown in some examples,that the outdoor air entering the underhood compartment to cool it by convection can warm up some components, such as the cold box, which is a “critical” component from a thermal point of view since it contains the car’s computers. This problem results from the architecture of the real underhood, specifically the positioning of these components downstream of and in the same air stream as warmer components. Passive control of thermal management can be achieved by placing these components in areas further upstream, or by isolating them from the hot air flow using deflectors. Note that for decreasing convective heat flux, it is essentially the early part of the transitional curve that causes this problem, since the convective heat flux can be as much as five times its asymptotic value. One can also implement an active control by using mobile deflectors to cut off the air flow towards the components in the transitory period, and let the air pass in the stabilized heat flux phase. This air can be useful for cooling other components around or downstream which are at higher temperatures. The deflector can be controlled by convective heat flux sensors.

Finally, an new underhood control procedure is presented that involves implementing in the actual car underhood static and mobile deflectors in order to protect certain components from hot air circulation. These deflectors can also direct cooling of the warm air passing over the low-temperature components towards the higher-temperature components. The new procedures proposed here are simple and easy to implement in the car underhood and are based essentially on the physical analysis obtained from temperature and separate convective and radiative heat flux measurements. For example, a dynamic open –closed deflector leaves the air passing over (or through) two components in the transitory phase but closes in the stabilized phase, when the first component in the airflow absorbs an increasing positive convective flux and the second one absorbs a decreasing (in absolute value) negative convective flux.

REFERENCES

[1] Weidmann, E.P., Widemann, J., Binner, T., Reister H. Underhood Temperature Analysis in Case of Natural Convection, SAE Paper 2005-01-2045, 2005

[2] Fournier, E., Bayne, T., Underhood Temperature Measurements of Four Vehicles, Motor Vehicle Fire Research Institute, Biokinetics and Associates, Ltd., Report R04-13, 2004

[3] Fournier, E., Bayne, T., Assessment of Thermocouple Attachment Methods for Measuring Vehicle Exhaust Temperature, Motor, Vehicle Fire Research Institute, by Biokinetics and Associates, Ltd., Report R06-23b for MVFRI, 2006

[4] Fournier, E., Bayne, T., Underhood Temperature Measurements, SAE Paper 2007-01-1393, 2007

[5] Jones, M. R., Fletcher, D. W., Thermal Performance Prediction of Front-End Heat-Exchange Modules, SAE Paper 2001-01-1765, 2001

[6] Francois, N., Using CFD for Heat Exchanger Development and Thermal Management, Valeo Engine Cooling, European Automotive CFD Conference EACC, Frankfurt, Germany, June 29-30, 2005

[7] Xiao, G., Investigation of Conjugate Heat Transfer for Vehicle Underbody, SAE Paper 2008-01-1819, 2008

[8] W. Ding, J. Williams, D. Karanth and S.D. Sovani, CFD Application in Automotive Front-End Design, SAE Paper 2006-01-0337, 2006

[9] F. Fortunato, F. Damiano, L. Matteo and P. Oliva, Underhood Cooling Simulation for Development of New Vehicles, SAE Paper 2005-01-2046, 2005

[10] S. Kini and R. Thoms, Multi-domain Mesches for Automobile Underhood Applications, SAE Paper 2009-01-1149

[11] Bailly, O., Baby, X., Fares, E., and de Portzamparc, H., PIV and Numerical Correlations on the Laguna II Underhood Flow Field, Renault, Congrès de la société des ingénieurs de l'Automobile SIA, Lyon, France, October 26-27, 2005

[12] Yang, Z., Bozeman, J., Shen, F.Z., CFD for Flow Rate and Air Recirculation at Vehicle Idle Conditions, General Motors Corporation, SAE Paper 2004-01-0053, 2004

[13] Jerhamre, A., Jönson, A., Development and Validation of Coolant Temperature and Cooling Air Flow CFD Simulations at Volvo Cars, Volvo Car Corporation, SAE Paper 2004-01-0051, 2004

[14] Weidmann, E.P., Reister, H., Binner, T., Experimental and Numerical Investigations of Thermal Soak, SAE Paper 2008-01-0396, 2008

[15] Hormann, T., Lechner, B., Puntigam, W., Moshammer, T., Aimbauer, R., Numerical and Experimental Investigation of Flow and Temperature Fields Around Automotive Cooling Systems, SAE Paper 2005-01-2006, 2005

[16] M. Khaled, F. Harambat, H. Peerhossaini, Véhicule Automobile à Ecoulement d'Air de Refroidissement optimisé, French patent application filed on January 20 2009, Patent n°1050365

[17] M. Khaled, F. Harambat and H. Peerhossaini, A quantitative method for the assessment of car inclination effects on thermal management of the underhood compartment, J. Thermal Science and Engineering Applications, ASME, 1 (2009) 014501: 1-5

[18] M. Khaled, F. Harambat and H. Peerhossaini, Temperature and heat flux behavior of complex flows in car underhood compartment, Heat Transfer Engineering, (2010), doi: 10.1080/01457631003640321

[19] M. Khaled, F. Harambat and H. Peerhossaini, Effects of car inclination on air flow and aerothermal behavior in the underhood compartment, Proceedings of the ASME Fluids Engineering Conference, July 30-August 2, San Diego, CA, USA (2008), FEDSM2008-55093

[20] M. Khaled, F. Harambat and H. Peerhossaini, Underhood thermal management: Temperature and flux measurements and physical analysis, Applied Thermal Engineering, 30 (2009) 590-598

[21] RC01 Radiation / Convection (RADCON) Heat Flux Sensor, HUKSEFLUX™ THERMAL SENSORS brochure

[22] M. Khaled, B. Garnier, F. Harambat, H. Peerhossaini, A New Method for Simultaneous Measurement of Convective and Radiative Heat Flux in Car Underhood Applications, Measurement Science and Technology Journal (2010), doi:10.1088/0957-0233/21/2/025903

[23] M. Khaled, F. Harambat, Dispositif de Mesure de Flux Thermique et Méthode de Séparation des Flux Radiatif et Convectif, French patent application filed on February 10 2009, Patent n°0950799